Schottky Tunnel Contacts for Efficient Coupling of Photovoltaics and Catalysts

Investigators
Paul C. McIntyre, Professor, Materials Science and Engineering
Christopher E.D. Chidsey, Associate Professor, Chemistry

Research Personnel
Andrew Scheuermann, Ph.D. Candidate (3rd year), Materials Science and Engineering
Olivia Hendricks, Ph.D. Candidate (2nd year), Chemistry

Abstract

This interdisciplinary project investigates the performance of nanoscale metal-insulator-semiconductor (MIS) contact structures that electrically couple optimized catalysts to high quality semiconductor absorbers in photoelectrochemical (PEC) cells, while chemically protecting the absorbers from oxidation during solar-driven water splitting.

In the 2013-14 funding period, we completed and published a study on water oxidation performance of varying the TiO_2 thickness (grown by atomic layer deposition – ALD) in the MIS structures.[1] Uniform films of atomic layer deposited TiO_2 are prepared in the thickness range ~1-12 nm on degenerately-doped p^+-Si yielding water oxidation overpotentials at 1 mA/cm^2 of 300 mV to 600 mV in aqueous solution (pH 0 to 14). Electron/hole transport through Schottky tunnel junction structures of varying TiO_2 thickness was studied using the reversible redox couple ferri/ferrocyanide. The dependence of the water oxidation overpotential on ALD-TiO_2 thickness, with all other anode design features unchanged, exhibits a linear trend corresponding to ~21 mV of added overpotential at 1 mA/cm^2 per nanometer of TiO_2 for TiO_2 thicknesses greater than ~ 2 nm. This linear behavior for anodes with thicker TiO_2 layers suggests bulk-limited electronic conduction through the insulator stack. A model of the field needed for bulk-limited transport at the given current densities agreed quantitatively with the experimental results lending further evidence for this hypothesis. Additionally, we have shown that ALD-TiO_2 protection can be used with three times less iridium with only small effects on device performance as well as with a variety of other metal catalysts.[1] These findings together constitute a major advance in the coupling of general photovoltaic and catalyst systems. In light of our findings of the bulk-limited conduction through thicker TiO_2 oxide layers, we recently performed another set of experiments varying the SiO_2 oxide thickness. An understanding of the tunnel oxide SiO_2 layer in coordination with an understanding of the ALD-TiO_2 layer will allow for better control of the overall stack conductivity and stability.

We have also assembled a new ALD reactor to investigate precursor chemistries for deposition of RuO_2-TiO_2 alloy layers that combine the capabilities of an efficient oxygen evolution reaction (OER) catalyst and a chemical protection layer for an underlying silicon absorber. Our goal is to minimize utilization of RuO_2, a rare, but very efficient,

OER catalyst. The new reactor has been optimized for TiO_2 deposition, and we will soon begin RuO_2 depositions from various ruthenium precursors.

Introduction

In this GCEP program, we investigate and apply our recently demonstrated approach[2] for protecting otherwise-unstable semiconductor surfaces in aqueous electrolytes to achieve efficient and stable photoelectrolysis of water using crystalline and amorphous, earth abundant semiconductors. Atomic layer deposition can be used to synthesize ultra-thin and pin-hole free TiO_2 films that allow facile carrier transport from a Si anode to an overlying nanoscale metal catalyst/electron transfer mediator.[2] Without the ALD-grown layer, a Si anode rapidly oxidizes destructively during water oxidation. The $Ir/TiO_2/SiO_2/Si$ nanocomposite anodes function as Schottky tunnel junctions at small insulator thicknesses. The ALD-grown TiO_2 insulator and SiO_2/Si interface avoid pinning of the silicon Fermi level that would otherwise occur at a metal/silicon interface.

Our ongoing research will use ALD to grow chemically protective oxide layers and form Schottky tunnel contacts on several different earth-abundant semiconductors. We will study the efficiencies of photovoltaic energy conversion and photosynthetic production of hydrogen and oxygen from water with optimized catalysts. Of particular interest is a photoelectrochemical cell using stable Schottky tunnel contacts to both a photoanode and photocathode, thus providing two photovoltages in series to drive the device. This can constitute a ***much simpler-to-fabricate two-junction solar cell***, more suitable for ***large-scale application*** than solid state multijunction cells, but using the same principle of selective absorption of different portions of the solar spectrum by semiconductors with different bandgaps. Closely coupling of experimental capabilities in the two PI's laboratories helps us establish the design rules, fabrication methods and photoelectrochemical performance of single-junction and two-junction PS and PV devices employing nanocomposite Schottky tunnel contacts. Our goal is to demonstrate simultaneous protection of the respective semiconductors from oxidation/dissolution while achieving unpinned Fermi levels in the semiconductors, rapid electronic transport across the oxide layer and highly efficient electrocatalysis at the oxide-electrolyte interface.

Background

In the past year, there have been an increasing number of published studies on ALD protection for photoelectrochemical applications as well as alternative catalysts that combine elements of stability. Three of these studies are particularly relevant to our work. Hu et al.[3] reported on thick ALD-TiO_2 films to stabilize Si, GaAs, and GaP. These films of thickness 4 to 143 nm were found to be highly conductive and relatively protective of the underlying semiconductors. One possible reason for their electronic conductivity is possible metal catalyst diffusion into the surface layer. It was found that a resistive surface layer was formed at the surface of the as-deposited ALD-TiO_2 film, and that this could be removed by etching or chemically modified by nickel deposition, whereby the nickel would partially intermix with the underlying TiO_2. These films were only conductive before post-catalyst annealing, and became highly insulating and no longer protecting the substrate after forming gas (H_2/N_2) anneals at temperatures between 350 and 600˚C. This recent study of TiO_2 layers of varying thickness by Hu et al. are in

the spirit of our own recently published research, in which we showed that TiO_2 layers greater than ~ 2 nm thick could be used with little penalty to photoelectrochemical efficiency. Our results suggested that bulk-limited conduction occurs for TiO_2 films thicker than ~ 2 nm through a spectrum of trap states with energies ~ 1 eV below the TiO_2 conduction band edge. The work of Hu et al. lends further evidence to our hypothesis that the bulk ALD-TiO_2 conductivity can be tuned, resulting to produce photoelectrochemical cells that operate at low overpotential with increased stability.

Another interesting study was reported by Kenney et al., who used thin films of electron beam evaporated nickel to protect n-Si photoanodes.[4] Nickel is a known earth-abundant catalyst for the oxygen evolution reaction, though like other reported earth-abundant catalysts, it is not stable under acidic conditions. The Ni film thickness was varied from 2 to 20 nm, and it was found that the MIS Schottky junction produced bya ~ 2 nm NiO_x/Ni layer on a SiO_x/n-Si photoanode afforded a photovoltage of approximately 500 mV in 1.0 M KOH. Increasing the thickness of the Ni film to 5 nm caused the photocurrent onset potential to increase by 300 mV, but no further increases were observed for thicker films. Perhaps most importantly, a 2 nm film of NiO_x/Ni was able to protect an underlying n-Si substrate for up to three days in a K-borate/Li-borate electrolyte solution. The authors hypothesized that this alternative electrolyte prevented further oxidation of the Ni during anodization, enhancing long-term stability.

Finally, McCrory et al. studied and compared a variety of earth-abundant catalysts for the oxygen evolution reaction.[5] Their goal was to provide a set of standardized criteria for evaluating and comparing various catalyst materials. The overpotential required to achieve 10 mA/cm^2, the necessary current density for a 10% efficient solar water-splitting device under 1 sun illumination, was chosen as the primary benchmark. Rotating disk voltammetry, rotating ring-disk voltammetry, and controlled current electrolysis were also used to study the catalytic activity, faradaic efficiency, and stability of the various catalysts over time. Based on their analysis, $NiFeO_x$ was identified as a promising earth-abundant catalyst; however, they noted that none of these earth-abundant catalysts approached the activity of their noble-metal counterparts. Therefore, much work is needed to improve the activity and stability of earth-abundant catalysts for water oxidation.

Results

The thickness of the ALD-TiO_2 is a key parameter for the performance of protected MIS Schottky anodes for water oxidation. We began the last year by completing and publishing the results of an investigation of the relationship between this ALD-TiO_2 thickness and the required overpotential to drive a 1 mA/cm^2 through an electrochemical cell during water splitting.[1]

Titanium dioxide layers were deposited by ALD on Si (100) wafers coated with ~1.5 nm of a chemical oxide (SiO_2) layer as-received from the wafer vendor. The TiO_2 film thickness ranged from 1.2 nm to 11.6 nm. The TiO_2 thickness was measured using a Gaertner ellipsometer calibrated by cross-sectional transmission electron microscopy (TEM) analysis. TEM results for TiO_2 layers of thickness ~2, 5, and 12 nm, respectively, are shown in Figure 1, indicating a uniform and continuous film with no evidence of the

catalyst layer mixing into the TiO_2 layer that would provide an alternative mechanism to transfer charge through the insulating oxide layers of the anode. Another indication of reliable ALD depositions is a stable growth rate. Over the entire thickness series investigated, the mean growth rate variation was less than 0.1Å/cycle. The reproducibility and uniformity of this deposition technique indicates the promise of using ALD for electrochemical device applications, where both very thin and uniform films are required.

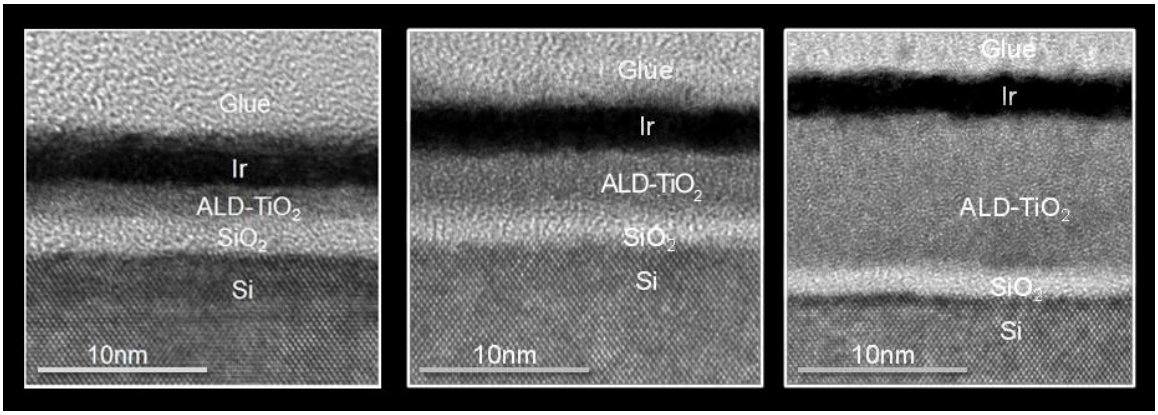

Figure 1: Transmission electron micrographs of three ALD-TiO_2 films of thickness 2 nm, 5 nm, and 12 nm from left to right.

Increasing the thickness of the ALD-grown TiO_2 oxide layer is expected to decrease the charge transfer efficiency of the anode, indicating the importance of an ultrathin layer for facile electronic carrier transport between the oxygen evolution catalyst and the semiconductor absorber. Indeed, the overpotential for water-oxidation required for devices to operate at 1 mA/cm^2 increases with increasing TiO_2 thickness for thicknesses greater than ~ 2 nm. Interestingly, the overpotential is relatively constant, at a value of 300 mV to 350 mV, for anodes with 0 to 2 nm of ALD-TiO_2, suggesting that the thickness of TiO_2 is not rate-limiting for the water oxidation reaction in this oxide thickness regime.

As shown in Figure 2, there are two distinct regimes: (1) From 0 to ~ 2 nm, where the trend is relatively independent of thickness and (2) from ~2 nm to 12 nm where the trend is linear with a slope of ~21 mV/nm of TiO_2, interestingly similar to the slope observed for the half peak-to-peak splitting of the ferri/ferrocyanide redox cyclic voltammograms. The conduction mechanism for ultrathin TiO_2, the first thickness regime, was previously indicated as direct tunneling, supported by the temperature independence of the conductivity, while anodes with thicker TiO_2, characteristic of the second regime in Figure 2, show a clear temperature dependence suggesting a more bulk limited, thermally-activated conduction mechanism.[1] Through this recent work and an investigation of the band diagram of the bilayer oxide TiO_2/SiO_2, this bulk-limited conduction mechanism has been further explicated, showing that a linear trend is expected with the slope equal to the characteristic value of the field in the TiO_2 needed to

drive 1 mA/cm^2. Taking the slopes in Figure 2, this corresponds to a field of 200-250 kV/cm and an effective ALD-TiO_2 resistivity of 1-2 × 10^8 Ω•cm.

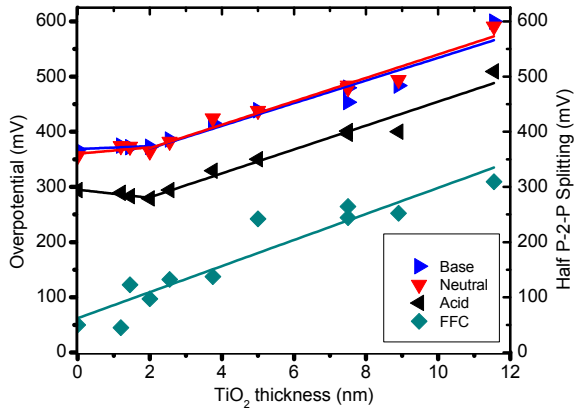

Table I: Linear regression analysis data for measured overpotentials as a function of TiO_2 thickness in all four solvent systems.

Solvent system	Linear slope (mV/nm of TiO_2)	Linear correlation (R^2)
Base	20.6	0.92
Neutral	21.2	0.97
Acid	21.7	0.96
FFC	23.6	0.90

Figure 2: Left: Overpotentials for water oxidation at 1mA/cm^2 and ferri/ferrocyanide half peak-to-peak splitting as a function of TiO_2 thickness. Table I gives the results of the corresponding linear regression analysis of these four trends. For water oxidation, the linear regression is applied to the regime from 2 nm to 12 nm of TiO_2.

In summary, the key findings are that 1) total overpotentials are quite low for these ALD-grown MIS anode structures, and 2) the overpotential penalty per nanometer of added TiO_2 thickness (e.g. for increased chemical stability) is modest. For ALD-TiO_2 thicknesses greater than ~2.0 nm, the effective overpotential for water oxidation increases linearly as the TiO_2 thickness is increased in accordance with a bulk-limited conduction mechanism that requires a characteristic E-field in the TiO_2 layer to maintain a given water oxidation current across the metal-insulator-semiconductor anode. For ultrathin TiO_2 films in which direct tunneling can dominate charge transport, the minimum overpotential and reaction rate are relatively independent of TiO_2 thickness and are apparently dominated by the kinetics of the water oxidation on the catalyst surface.[1]

In addition to this study of ALD-TiO_2 thickness, we performed solid-state and photoelectrochemical analyses on anodes with different metal catalysts. It was found that reducing the thickness of iridium even three-fold had very little effect on the overpotential, indicating the possibility to reduce costs with a minimal effect on device performance. More broadly, changing the catalyst is anticipated to have two primary effects on the performance of a Schottky junction photoanode device: 1) altering the built-in potential essential for separating the photo-generated excitons by changing the catalyst work function, and 2) altering the water oxidation kinetics by changing the nature of the catalytic site. If the Fermi level in such a device were pinned, the photovoltage could no longer be manipulated to improve device performance. A photovoltage of 550 mV, observed in our previous experiments, strongly suggests an un-pinned Fermi level at the tunnel oxide-protected Si surface. By changing the gate metal in MIS capacitors and observing near-ideal flat band voltages independent of identity of the metal, our experiments provide further evidence that addition of an ultrathin ALD-TiO_2 layer to the

MIS anode structure does not pin the Fermi level at the Si surface. Evidence of an un-pinned Fermi level with the ability to use different catalyst materials coupled with the low tradeoff in conductivity for thicker stabilization layers is a major development.[1]

Table II: Half peak-to-peak splitting in ferro/ferri cyanide (FFC) voltammograms and overpotentials at 1 mA/cm^2 for water oxidation for catalyst layers on 2 nm of TiO_2 on SiO_2/p^+-Si.

Catalyst layer	FFC half splitting (mV)	1 M Acid (mV)	1 M Phosphate Buffer (mV)	1 M Base (mV)
1 nm Ir	80	300	311	340
2 nm Ir	70	282	319	337
3 nm Ir	60	265	316	343
3 nm Ru[a]	95	265	383	-
2 nm Pt	85	469	628	575
2 nm Au[b]	60	1160	1120	790
2 nm Co	> 500	885	966	937
2 nm Co + CoPi[c]	> 500	817	730	1061

More recently, results obtained from n-Si photoanodes in the light have shown an interesting dependence of the measured photovoltage on the ALD-TiO_2 thickness. The photovoltage was observed to increase with decreasing ALD-TiO_2 thickness even though the dark reverse saturation current increased in current-voltage measurements – often thought to lead to increasing recombination and therefore lower photovoltage. MIS capacitance analysis was performed on devices with varying TiO_2 thickness before and after forming gas anneal to probe for the presence of fixed charge in the insulator layers that could explain this apparent photovoltage trend. The result shown in Figure 3 below indicate a constant V_{fb} with TiO_2 thickness, implying that fixed charge was not responsible for the voltage difference.

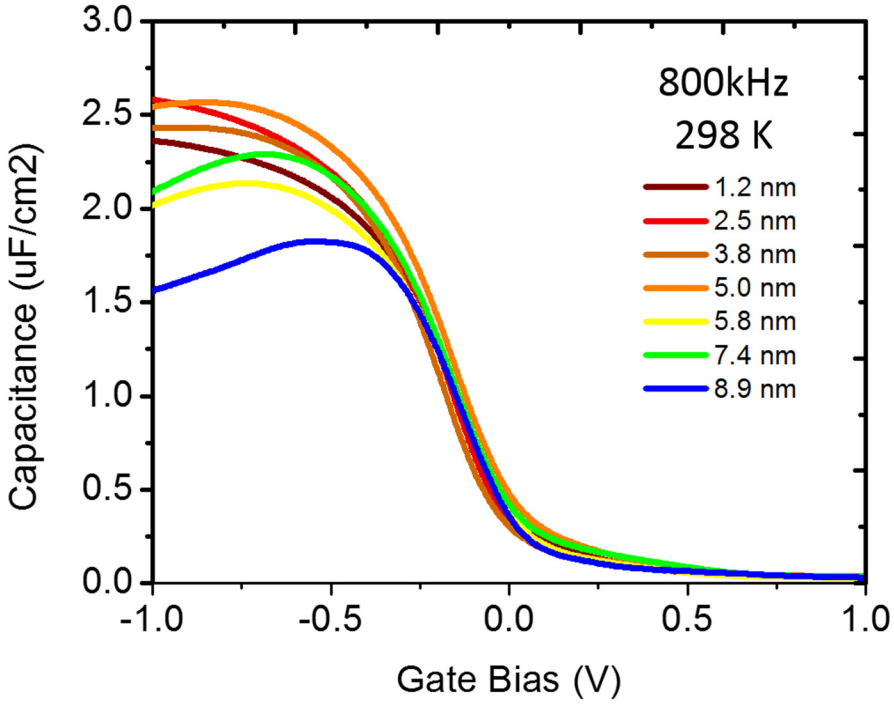

Figure 3: Capacitance-voltage curves of 50nm Ir/'x' nm ALD-TiO_2 / 1.5nm SiO_2 / pSi devices taken at 800 kHz and room temperature. The curves fall within tens of millivolts of one another in the flat band voltage regime indicating that fixed charge does not contribute significantly to the flat band voltage (and, thus, the photovoltage) of these MIS structures.

To better understand the relationship between the photovoltage of MIS cells for photoelectrochemistry and the protecting insulator layers, we studied devices with changing TiO_2 and SiO_2 layers. The ALD-TiO_2 now understood to be a resistive oxide at higher thickness was expected to play a different role than the ultrathin, chemical SiO_2 layer believed to act as a tunnel junction in series with the TiO_2. SiO_2 layers were grown in the range of 1.5 to 11.5nm by the Slot Plane Antenna (SPA) plasma method established by Tokyo Electron Limited. This method allows for controlled growth of SiO_2 layers at temperatures below 400C due to the high concentration of oxygen radicals formed by the plasma. The resulting films were used to study the photoelectrochemical performance of Ir/SiO_2/Si anodes as a function of SiO_2 thickness. The anodes showed an exponential dependence of the resistance on thickness as expected for quantum tunneling.

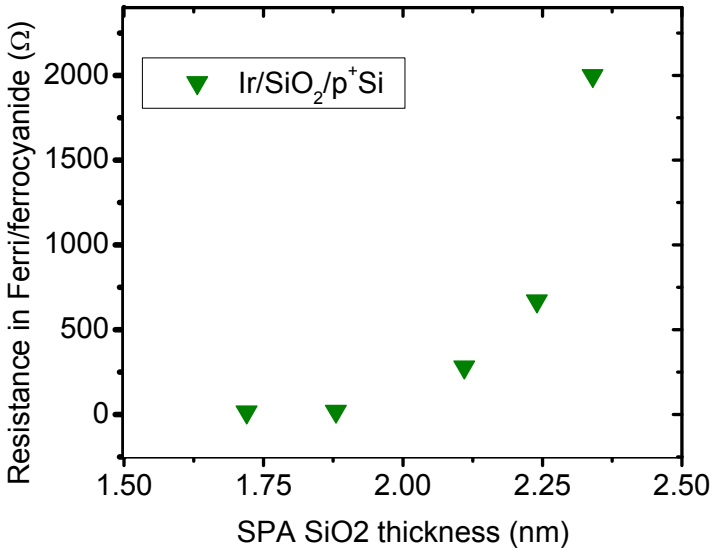

Figure 4: Modeled series resistance of Ir/'x'nm SiO_2/p^+Si anodes from the experimentally obtained cyclic voltammograms in ferri/ferrocyanide. The data follow an approximately exponential trend with thickness, as expected for quantum tunneling.

The photovoltage was observed to increase with decreasing SiO_2 thickness, however, similarly to the ALD-TiO_2 case, and not in accordance with the reverse saturation current. Another experiment was conducted changing the SiO_2 thickness in $Ir/TiO_2/SiO_2/Si$ anodes with the SPA method to study the dynamics of changing the tunnel oxide thickness in the actual structure of interest. Here again, an approximately exponential dependence of resistance on SiO_2 thickness was observed and an increasing photovoltage with thinner films. Finally, we are in the process of fabricating and characterizing anodes with ALD-Al_2O_3, also believed to act as a tunnel junction as opposed to a resistive oxide, but with a different dielectric constant. The results of these experimental studies are being combined with theoretical modeling using the Sentaurus software package. Together, these should provide insights on the tradeoffs and advantages of different tunnel oxide and resistive oxide combinations for photoelectrochemical cells.

As the scheme of using protective oxides for photoelectrochemical devices in MIS configurations gains in popularity, deeper understanding of the junction physics becomes increasingly important and our work on this GCEP program should provide crucial understanding.

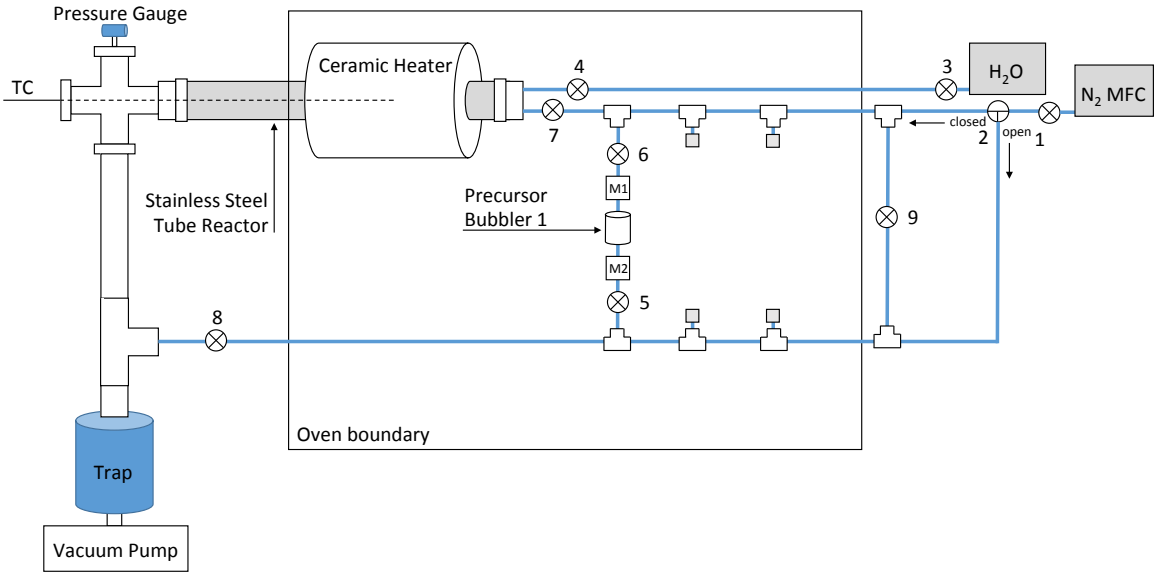

Figure 3: Schematic of new ALD reactor.

A second major research effort involves developing optimal catalysts for the oxygen evolution reaction. Noble metals such as ruthenium, iridium, and their oxides are the most efficient catalysts for water oxidation.[6] Given their high cost, however, it is important to understand how these noble metals can be most efficiently and effectively used. We plan to investigate ALD surface alloying of RuO_2 with TiO_2. By decorating the TiO_2 surface with Ru ions at an optimal areal density, we hope to optimize the turnover frequency for oxygen evolution by achieving surfaces with the same electrocatalytic current density as planar 2D catalyst layers, but with a fraction of the noble metal usage.

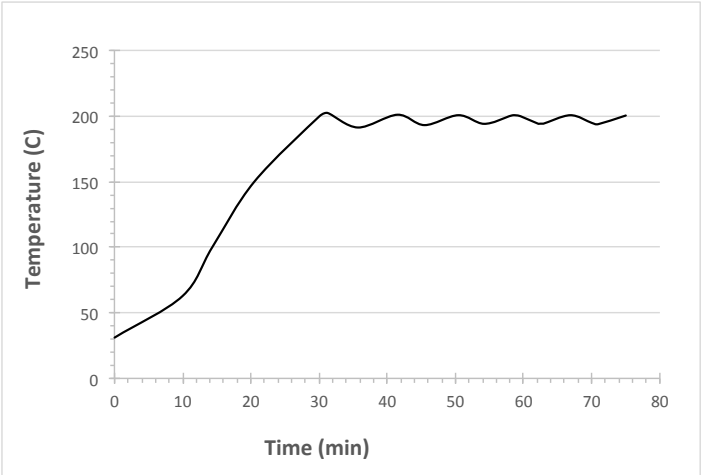

Figure 4: Deposition chamber temperature as a function of time for optimized temperature control.

In order to rapidly screen novel precursors, we designed a new, customized ALD reactor specifically for this purpose. The schematic of the completed reactor is shown in Figure 3. The system can accommodate up to three different precursors. An Edwards pump is used to maintain a base pressure of approximately 18 mTorr, as measured by a convection pressure gauge. The deposition chamber is a 1.5" OD stainless steel tube encased in a ceramic heater with temperature capabilities of up to 980 °C. The

temperature inside the stainless steel tube reactor is controlled by a type-K thermocouple and an Omega CNi3222 temperature controller. As shown in Figure 4, a stable temperature is reached within 25 minutes and temperature stability is within ± 5 °C at a set point of 200 °C. Figure 5 shows the temperature profile for the stainless steel reactor. Less than 10 °C variation is achieved between 3.5-5 in. inside the heater. Precursors are housed in stainless steel bubblers designed with three ports: an inlet for carrier gas flow, an outlet for delivery to the chamber, and a final port for filling. A 3-way switching valve directs the flow of nitrogen gas directly into the chamber, as during a purge pulse, or through one of the bubblers, as during a precursor pulse. A 100 sccm mass flow controller determines the flow rate of nitrogen gas. To maintain the precursor bubblers and lines at a constant temperature, the entire system is encased in a convection oven with temperature uniformity of ±1.8 °C at 150 °C. The valves are pneumatically actuated and rated to approximately 200°C, which allows precursors to be heated to higher temperatures than what is commonly seen in the literature. By placing nearly all of the system components within the oven, we can achieve enhanced temperature uniformity and easily control precursor vapor pressure. Overall, we have attempted to minimize system components in order to focus on the chemistry of ALD, rather than the process engineering.

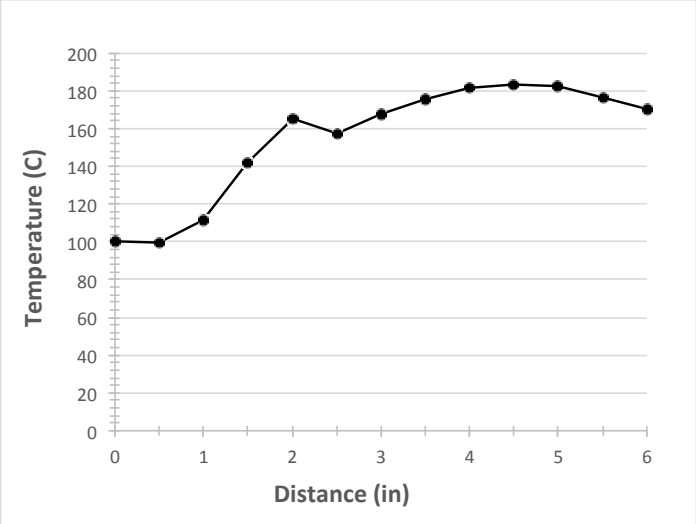

Figure 5: Temperature profile for the deposition chamber as a function of distance inside the heater.

We have tested our system with tetrakis(dimethylamino) titanium (TDMAT), a well-known ALD precursor for TiO_2 deposition that has been extensively studied in our lab.[7] The bubbler and lines are maintained at 70 °C, as thermogravimetric analysis has shown that liquid TDMAT begins to decompose at temperatures as low as 130 °C. The gas phase dissociation onset temperature, however, is much higher, and thus the deposition chamber is maintained at 170 °C. A typical ALD process is initiated by opening the manual valve M1. After the oven and deposition chamber temperatures have equilibrated, a computer code written in MATLAB is initiated that controls the pneumatically actuated valves. A summary of the ALD deposition process is shown in Table 1.

Step	Valves open	Time	Description
1a-equilibration	None	5 min	Evacuate main chamber
1b-equilibration	7	5 min	Evacuate precursor inlet line
1c-equilibration	2 and 8	5 min	Evacuate carrier gas line
2a-purge	1 and 7	5 min	Purge precursor inlet line
2b-purge	1, 2, and 8	5 min	Purge carrier gas line
3a-pump down	None	30 sec	Evacuate main chamber
3b-pump down	2, 8, and 9	30 sec	Evacuate carrier gas line
3c-pump down	8 and 9	30 sec	Evacuate precursor inlet line
4-water charge	3	5 sec	Open H_2O bubbler, fill water line
5-water pulse	4	0.5 sec	Pulse H_2O to main chamber
6a-purge	1, 8, and 9	15 sec	Purge precursor inlet line
6b-purge	1, 2, and 8	15 sec	Purge carrier gas line
6c-purge	1 and 7	15 sec	Purge main chamber
7a-pump down	None	15 sec	Evacuate main chamber
7b-pump down	2, 8, and 9	15 sec	Evacuate carrier gas line
7c-pump down	8 and 9	15 sec	Evacuate precursor gas line

7-TDMAT charge	6	5 sec	Open TDMAT bubbler and fill precursor gas line
8-TDMAT pulse	7	0.7 sec	Pulse TDMAT to main chamber
9a-purge	1, 8, and 9	15 sec	Purge precursor inlet line
9b-purge	1, 2, and 9	15 sec	Purge carrier gas line
9c-purge	1 and 7	15 sec	Purge main chamber
10a-pump down	None	15 sec	Evacuate main chamber
10b-pump down	2, 8, and 9	15 sec	Evacuate carrier gas line
10c-pump down	8 and 9	15 sec	Evacuate precursor gas line
11-cycle	Repeat steps 4-10 for the desired number of cycles		

With this procedure, consistent and uniform TiO_2 deposition was achieved with a growth rate of 0.5-0.6 Å/cycle for 50 and 100 cycle depositions. Table 2 summarizes the growth rate data for these depositions. To qualify these depositions as ALD, the chamber temperature was varied from 150 °C to 200 °C, keeping all other parameters the same. As shown in Figure 6, the growth rate remains constant from 150 °C to 180 °C, increasingly slightly at 190 °C and dramatically at 200 °C. This suggests that we are within the

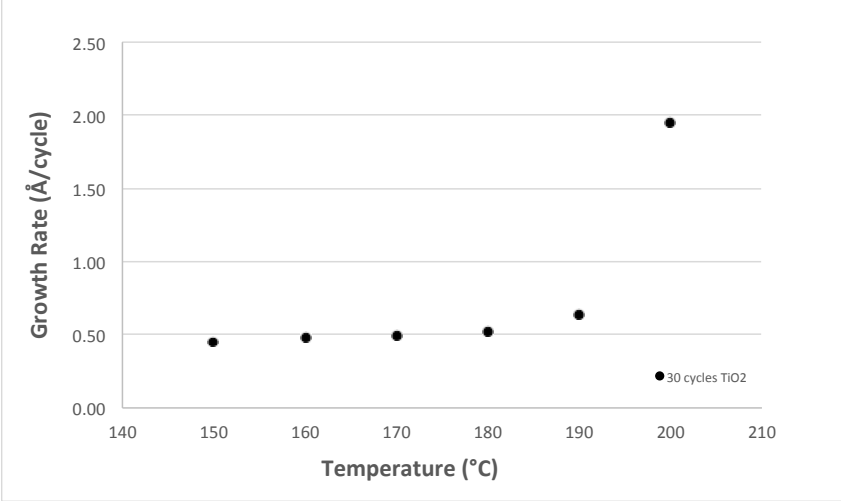

Figure 6: Growth rate as a function of temperature for 30 cycles TiO_2 deposition.

ALD window for 150-180 °C. To further qualify as ALD, a full thickness series will be performed, varying the number of cycles to confirm constant growth rate as a function of film thickness. In addition, both the TDMAT and H_2O pulse times will be varied to demonstrate saturated growth. After firmly establishing ALD TiO_2, we will optimize RuO_2 deposition from (2,4-dimethylpentadienyl)Ru(II) or variations of Ru(III) acetylacetonate.

Progress

Our observation of a conduction pathway through bulk defect states in the TiO_2 is exciting and suggests that stability of the underlying semiconductor absorber can be increased with only a modest penalty in device efficiency. Further, the utility of ALD-TiO_2 with a variety of metal catalysts suggests the potential to effectively engineer simultaneous chemical protection and efficient electrochemical kinetics for a variety of solar-fuel and solar-chemical applications. In contrast to our observations of bulk-limited conduction in devices with thick ALD-TiO_2, we have been able to observe the role of quantum tunneling through the SiO_2 layer by purposefully varying the SiO_2 thickness. A better understanding of the whole oxide stack will allow for future tuning of the conductivity and stability of the device. This is essential for making a viable PEC-based solar fuel synthesis technology incorporating high quality photovoltaic materials such as (normally unstable) Si, III-V and II-VI semiconductors. Further work on ALD catalysts layers and tuning the oxide conductivity and stability are underway.

Future Plans

A 2D-alloyed RuO_2/TiO_2 electrode represents a modern, ultra-thin analogue to the thick film dimensionally stable anodes (DSAs) used widely in industry for electrochemical chlorine synthesis. Alloys of RuO_2 and TiO_2 have previously been investigated for catalytic oxygen evolution, and based on those results, we expect maximum electrocatalytic activity per Ru atom near 30 mol% RuO_2.[8] To create ALD-grown alloys, we will vary the pulse cycles for each metal oxide between 0 and 100% to create electrocatalyst of varying composition.[9] Stanford hosts an impressive collection of instruments for materials characterization, including scanning electron microscopy, Rutherford backscattering, X-ray diffraction, X-ray reflectivity, and inductively coupled plasma atomic emission and mass spectroscopies. These techniques will allow us to fully characterize the surface structure and composition of the alloys. In addition, cyclic voltammetry (CV) will be used to study water oxidation current as a function of applied potential in the light and in the dark, as well as in acidic, basic, and neutral solutions. CV will also be used to characterize charge transport between ALD-grown RuO_2-TiO_2 alloys and standard redox couples in aqueous solution. Finally, chronoamperometry and chronopotentiometry will be used to monitor the lifetime of the resulting electrodes.

Once we understand how electrode composition affects electrocatalytic activity, we will attempt to template Ru ions at a fixed distance from one another using novel ruthenium precursors. We predict that hard-donor anionic oxygen ligands will be displaced by Ti-O bonds under the hydroxylic conditions of ALD, while neutral aromatic amine ligands will be preserved. Therefore, bridging amine ligands in a dinuclear ruthenium precursor could be used to separate two Ru atoms at a fixed distance during their incorporation into the alloyed catalyst. Our goal is to develop a ruthenium ALD

precursor that can yield templated dimeric Ru sites films using a milder oxygen source, such as H_2O, as opposed to oxygen gas. For example, a potential precursor will be prepared from ruthenium trisacetylacetonate and 2,2'-bipyrimidine.[10] The distance between Ru atom centers can be varied by using different bridging amines. After securely anchoring the Ru atoms in place, we will remove the bridging ligand by aggressive oxidation, for instance with an oxygen plasma. If successful, this strategy will allow us to determine the "ideal" Ru-separation for catalytic oxygen evolution. Precise control over Ru atom placement should yield enhanced catalytic activity compared to random alloys.

While progress has been made in understanding the mechanism of electronic carrier conduction through ALD-TiO_2 protected devices, little has been done to directly control the conductivity and stability. Additionally, the relationship between increasing conductivity across leaky TiO_2 and the effect of recombination on device photovoltage is not well understood. A more detailed understanding of these topics will allow us to tune the properties of the oxide interconnects between photovoltaics and catalysts allowing for high electrical efficiencies and robust chemical stabilities. Our planned experiments in this arena will include modifying the conductivity of the overall stack both through forming gas anneal targeting the ALD-TiO_2 layer and gettering and etching targeting the SiO_2 tunnel oxide. We will perform both solid-state and electrochemical cell measurements to determine the conductivity of the MIS structures and the respective photovoltages and stabilities that accompany these treatments. Finally, in the next year, we will focus more of our efforts on ALD-oxide protected photocathodes, with particular emphasis on amorphous Si thin film absorbers to provide much greater photovoltages in two-junction cells combined with crystalline Si Schottky junctions.

Publications and Patents

1) A.G. Scheuermann, J.D. Prange, M. Gunji, C.E.D. Chidsey, P.C. McIntyre. "Effects of Catalyst Material and Atomic Layer Deposited TiO_2 Oxide Thickness on the Water Oxidation Performance of Metal-Insulator-Silicon Anodes." *Energy & Environmental Science*, **6**, 2487-2496 (2013).
2) A.G. Scheuermann, J.P. Lawrence, M. Gunji, C.E.D. Chidsey, P.C. McIntyre. "ALD-TiO_2 Preparation and Characterization for Metal-Insulator-Silicon Photoelectrochemical Applications." *ECS Transactions*, 58(10), 75-86 (2013).

References

1. A.G. Scheuermann, J.D. Prange, M. Gunji, C.E.D. Chidsey, P.C. McIntyre. "Effects of Catalyst Material and Atomic Layer Deposited TiO_2 Oxide Thickness on the Water Oxidation Performance of Metal-Insulator-Silicon Anodes." *Energy & Environmental Science*, **6**, 2487-2496 (2013).
2. Chen, Y.W.; Prange, J.D., Duehnen, S., Park, Y., Gunji, M., Chidsey, C.E D. and McIntyre, P.C., "Atomic Layer-Deposited Tunnel Oxide Stabilizes Silicon Photoanodes for Water Oxidation," *Nature Mat.* **10**, 539-44 (2011).
3. S. Hu, M. Shaner, J. Beardslee, M. Lichterman, B. Brunshwig, N. Lewis. "Quantitative, Sustained, Efficient Solar-Driven Water Oxidation with "Leaky" TiO_2 Coatings." Accepted Manuscript *Science* (2014).
4. M.J. Kenney, M. Gong, Y. Li, J.Z. Wu, J. Feng, M. Lanza, and H. Dai, "High-Performance Silicon Photoanodes Passivated with Ultrathin Nickel Films for Water Oxidation," *Science* **342**, 836-40 (2013).
5. C.C.L. McCrory, S. Jung, J.C. Peters, and T.F. Jaramillo, "Benchmarking Heterogeneous Electrocatalysts for the Oxygen Evolution Reaction," *J. Am. Chem. Soc.* **135**, 16977 (2013).
6. G. Chen, D.A. Delafuente, S. Sarangapani, and T.E. Mallouk, "Combinatorial Discovery of Bifunctional Oxygen Reduction – Water Oxidation Electrocatalysts for Regenerative Fuel Cells,"

Catal. Today **67**, 539-44 (2011); J. Rossmeisl, Z.Q. Qu, H. Zhu, G.J. Kroes, and J.K. Norskov, "Electrolysis of Water on Oxide Surfaces," *J. Electroanalytical Chem* **607**, 83-9 (2007).
7. A.G. Scheuermann, J.P. Lawrence, M. Gunji, C.E.D. Chidsey, P.C. McIntyre. "ALD-TiO_2 Preparation and Characterization for Metal-Insulator-Silicon Photoelectrochemical Applications." *ECS Transactions*, 58(10), 75-86 (2013).
8. C.H. Comninellis and G.P. Vercesi, "Characterization of DSA® -Type Oxygen Evolving Electrodes: Choice of a Coating," *J. Appl. Electrochem.* **21**, 335-45 (1991).
9. J.W. Elam and S.M. George, "Growth of ZnO/Al_2O_3 Alloy Films Using Atomic Layer Deposition Techniques," *Chem. Mater.* **15**, 1020-28 (2003).
10. M.A. Bennett, M.J. Byrnes, and I. Kovacik, "The Fragment Bis(acetylacetonato)ruthenium: A Meeting-Point of Coordination and Organometallic Chemistry," *J. Organometallic Chem.* **689**, 4463-74 (2004).

Contacts

Paul C. McIntyre: pcm1@stanford.edu
Christopher E.D. Chidsey: chidsey@stanford.edu
Andew Scheuermann: awsch829@stanford.edu
Olivia Hendricks: ohendric@stanford.edu